

Designing Higher Resolution Self-Assembled 3D DNA Crystals via Strand Terminus Modifications

Yoel P. Ohayon,[†] Carina Hernandez,[†] Arun Richard Chandrasekaran,^{†,ID} Xinyu Wang,[†] Hatem O. Abdallah,[†] Michael Alexander Jong,[†] Michael G. Mohsen,[†] Ruojie Sha,^{†,ID} Jens J. Birktoft,[†] Philip S. Lukeman,^{§,ID} Paul M. Chaikin,[‡] Stephen L. Ginell,[‡] Chengde Mao,^{¶,ID} and Nadrian C. Seeman^{*,†,ID}

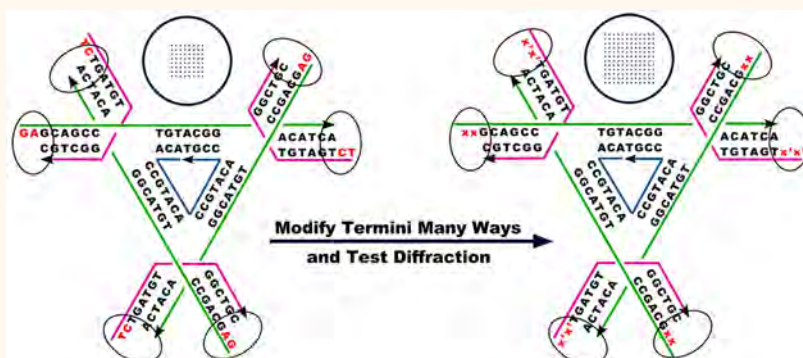
[†]Department of Chemistry and [‡]Department of Physics, New York University, New York, New York 10003, United States

[§]Department of Chemistry, St. John's University, New York, New York 11439, United States

[¶]Structural Biology Center, Argonne National Laboratory, Argonne, Illinois 60439, United States

^{*}Department of Chemistry, Purdue University, West Lafayette, Indiana 47907, United States

Supporting Information



ABSTRACT: DNA tensegrity triangles self-assemble into rhombohedral three-dimensional crystals via sticky ended cohesion. Crystals containing two-nucleotide (nt) sticky ends (GA:TC) have been reported previously, and those crystals diffracted to 4.9 Å at beamline NSLS-I-X25. Here, we analyze the effect of varying sticky end lengths and sequences as well as the impact of 5'- and 3'-phosphates on crystal formation and resolution. Tensegrity triangle motifs having 1-, 2-, 3-, and 4-nt sticky ends all form crystals. X-ray diffraction data from the same beamline reveal that the crystal resolution for a 1-nt sticky end (G:C) and a 3-nt sticky end (GAT:ATC) were 3.4 and 4.2 Å, respectively. Resolutions were determined from complete data sets in each case. We also conducted trials that examined every possible combination of 1-nucleotide and 2-nucleotide sticky-ended phosphorylated strands and successfully crystallized all 16 possible combinations of strands. We observed the position of the 5'-phosphate on either the crossover (1), helical (2), or central strand (3) affected the resolution of the self-assembled crystals for the 2-turn monomer (3.0 Å for 1–2P-3P) and 2-turn dimer sticky ended (4.1 Å for 1–2–3P) systems. We have also examined the impact of the identity of the base flanking the sticky ends as well as the use of 3'-phosphate. We conclude that crystal resolution is not a simple consequence of the thermodynamics of the direct nucleotide pairing interactions involved in molecular cohesion in this system.

KEYWORDS: DNA crystals, self-assembly, crystalline order optimization, sticky ends, terminal phosphates

Apart from DNA being well-known as the genetic material of living organisms,¹ synthetic branched DNA molecules can be used to build structures and devices on the nanometer scale.² It has been suggested that three-dimensional crystalline arrangements formed by deliberate self-assembly could be used to design 3D macroscopic species.³ Branched DNA motifs can be held together by sticky ended

cohesion,⁴ and the arms of the branches assume the well-known B-DNA structure on hybridization with complementary nucleotide pairs.⁵ Thus, well-structured branched DNA motifs

Received: March 28, 2019

Accepted: June 25, 2019

Published: June 25, 2019



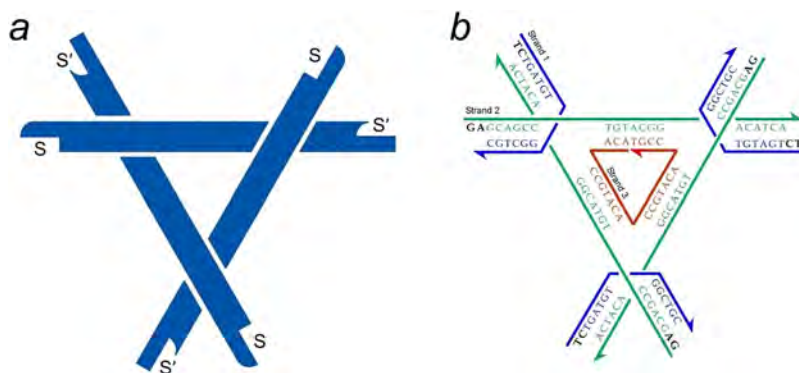


Figure 1. Schematic of a three-fold symmetric two-turn tensegrity triangle. (a) Illustration shows the over-and-under arrangement of double helices in the tensegrity triangle. The three edges are tailed by sticky ends that are complementary to the other end of the helix (sticky ends are denoted as S being complementary to S'). (b) Schematic design showing the 2-turn triangle from ref 7 with full sequences. Half arrowheads indicate the 3' ends of strands. Sticky ends (two nucleotides long) are shown in black letters.

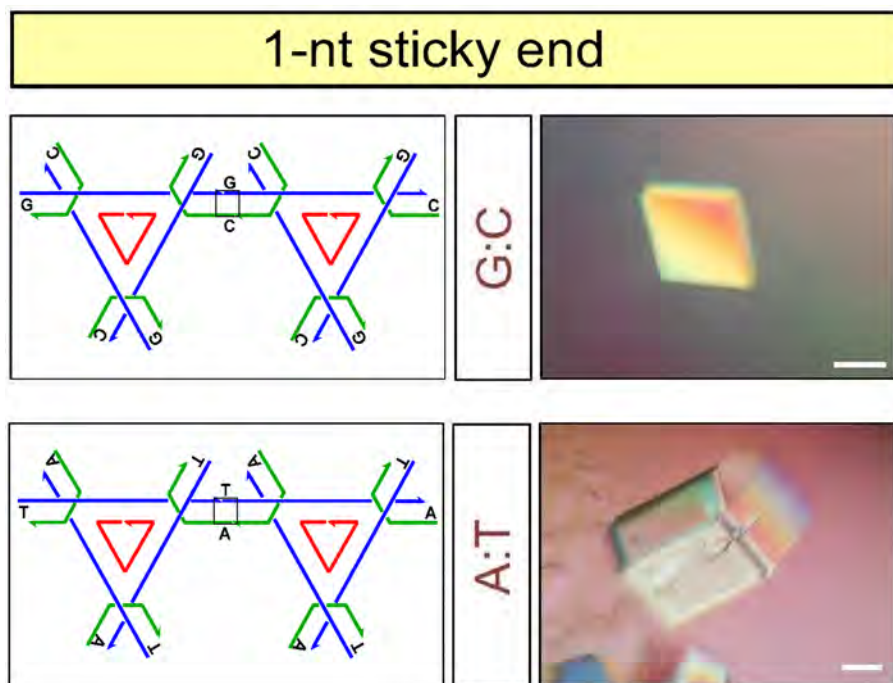


Figure 2. Crystals of the 2-turn triangle with 1-nucleotide sticky ends. The image shows the sticky end connectivity between two neighboring triangles (left) and the respective crystals obtained from each design (right). Scale bars are 100 μ m.

tailed by sticky ends are suitable for the construction of three-dimensional crystals. One such motif is the DNA tensegrity triangle, comprising three four-arm junctions, which can be tailed by sticky ends.⁶ We have reported previously a rationally designed, self-assembled, 3D crystal based on the DNA tensegrity triangle; this crystal diffracted to 4.0 \AA on beamline 19ID at the Advanced Photon Source (APS-Argonne National Laboratory, Argonne, IL, USA) and to about 5.0 \AA on a less brilliant beamline (NSLS-I-X25) at the National Synchrotron Light Source (NSLS-Brookhaven National Laboratory, Upton, New York, USA).⁷ The tensegrity triangle is a robust DNA motif with three-fold backbone rotational symmetry, consisting of three double helices that are directed along linearly independent directions. Figure 1a shows a schematic diagram of the tensegrity triangle. The three helical domains contain two double helical turns (21 nucleotide pairs, including sticky ends) and in this instance are three-fold symmetric (Figure 1b). There are three strands in the molecule, in a 3:3:1 ratio:

three that partake in the crossovers near the corners (strand 1, blue in Figure 1b), three that extend for the length of each double helix (strand 2, green in Figure 1b), and a final nicked strand at the center (strand 3, red in Figure 1b), completing the crossovers and the double helices between them. The helices are directed by sticky ends to cohere with six other triangles, thereby yielding a six-connected 3D crystalline arrangement. We have also reported two other self-assembled crystals based on the DNA tensegrity triangle. One of them was designed to contain two different triangles per asymmetric unit⁸ and the other one had three helical turns (31 nucleotide pairs) on each of its three edges.⁹ The first crystal diffracted to 5.0 \AA at beamline X6A at NSLS and the second crystal diffracted to 6.7 \AA at NSLS-I-X25.

Single crystals with molecular components held together by base pairing are rare^{5,10,11} unless they have been designed to cohere in this fashion. Designed crystals have long been regarded as a goal of structural DNA nanotechnology.³ Such

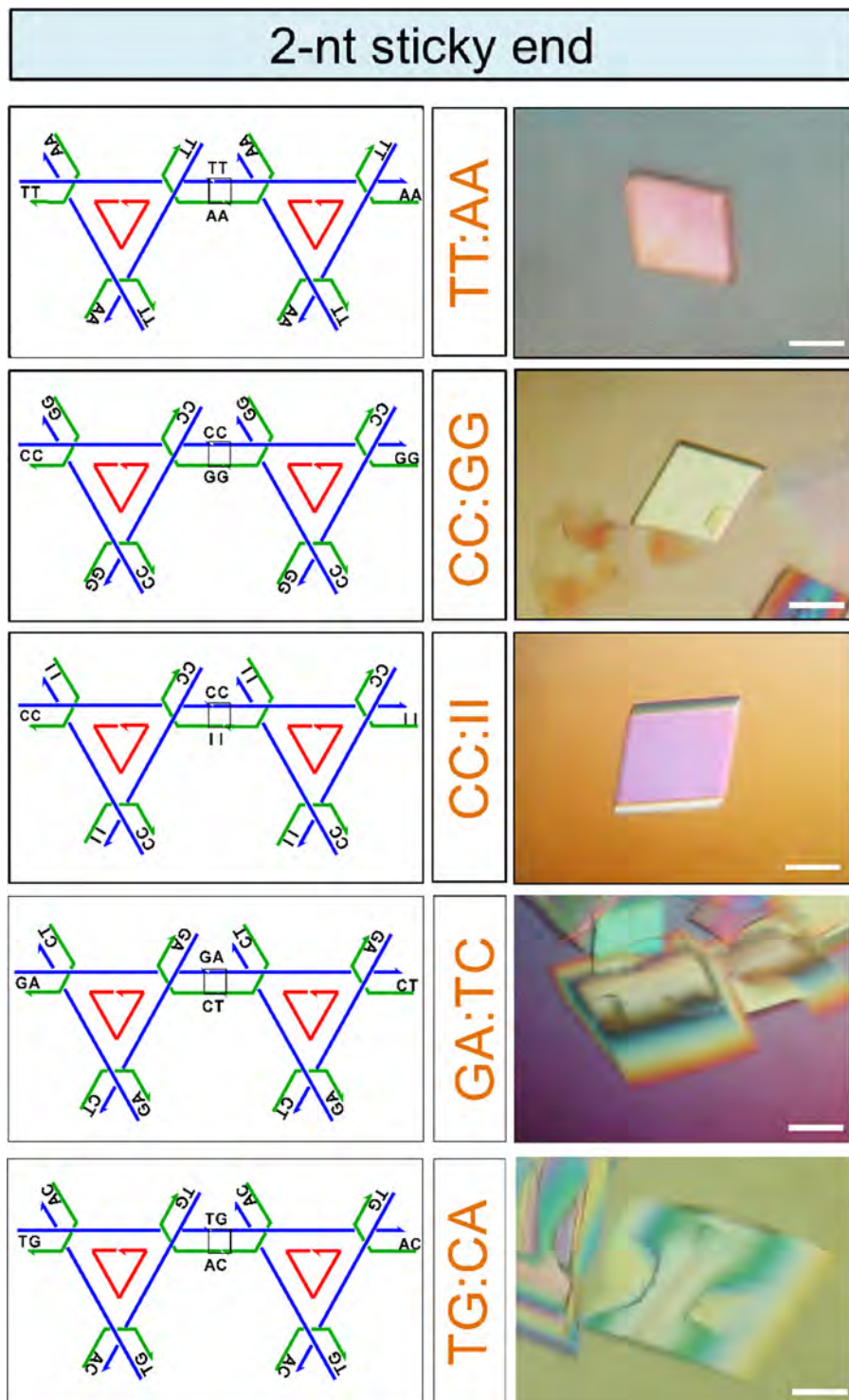


Figure 3. Crystals of the 2-turn triangle with 2-nucleotide sticky ends. The image shows the sticky end connectivity between two neighboring triangles (left) and the respective crystals obtained from the designs (right). Scale bars are 100 μ m.

3D crystalline nucleic acid systems have potential applications as scaffolds for crystallographic structure determination of biological systems² as well as for the organization of nanoelectronics.¹² The crystallographic application of scaffolding requires the highest possible resolution, and we are examining parameters that might enable us to improve the resolution obtained for these structures. We recently reported that addition of 5'-phosphates to the DNA strands improved resolution to 4.1 \AA at beamline NSLS-I-X25¹³ when the sticky

ends contained two nucleotides. This current study aims to analyze the effect of sticky end length and sequence on crystal formation and resolution as well as the effect of the bases that flank the sticky end and the presence of both 5'- and 3'-phosphates. Resolution was established from complete data sets for each crystal. A related study of sequence variation in two-turn tensegrity triangle crystals using only still photographs has been reported recently by Dietz and his colleagues.¹⁴ As a consequence of the complete-data set

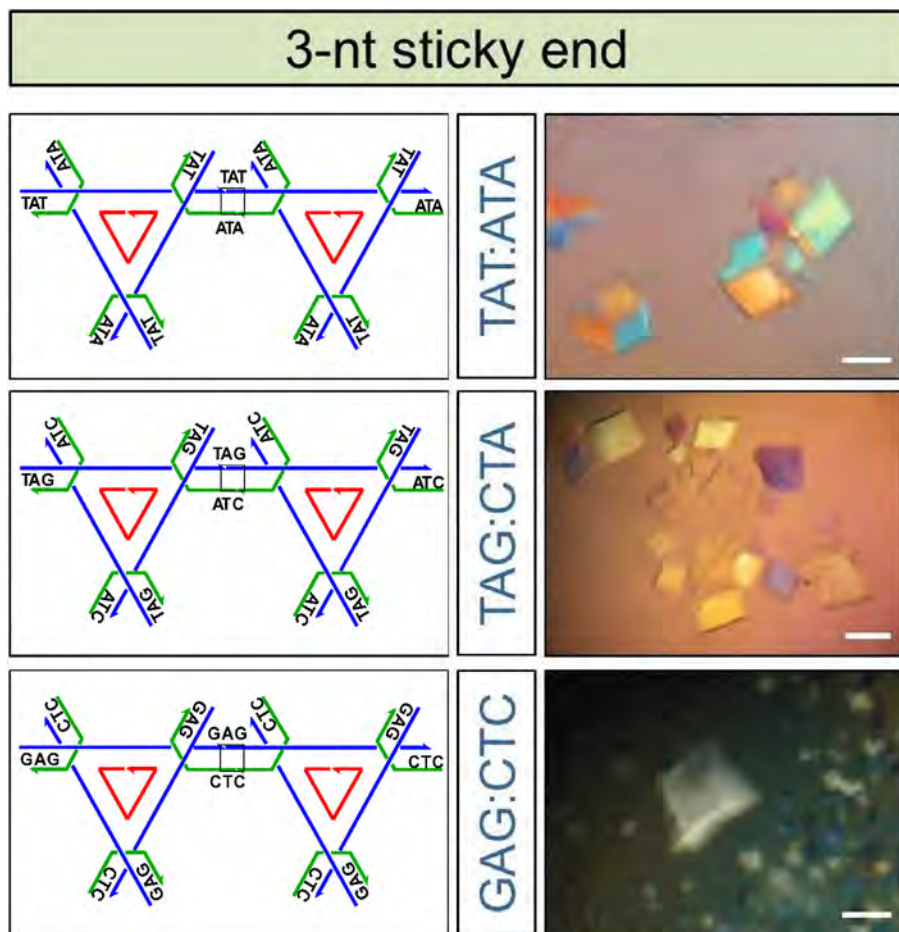


Figure 4. Crystals of the 2-turn triangle with 3-nucleotide sticky ends. The image shows the sticky end connectivity between two neighboring triangles (left) and the respective crystals obtained from the designs (right). Scale bars are 100 μ m.

approach taken here, we have not examined more than a single crystal for each of the systems described.

RESULTS AND DISCUSSION

Effect of Sticky End Length and Sequence. We were able to crystallize the 2-turn tensegrity triangle motif with 1-nt, 2-nt, 3-nt, and 4-nt sticky ends in every case attempted; the sticky end structures and their respective crystals are shown in Figures 2–5. Crystallization procedures are described in the *Methods*. After crystals were flash frozen by immersion into liquid nitrogen, X-ray diffraction data were collected at beamline NSLS-I-X25. In all cases but two, the triangles crystallized in the designed space group R3. The two exceptions (both P3₁) involve [1] a single A sticky end designed to pair to a T and [2] a GG designed to pair to a CC. The first case has numerous ways of pairing. In work to be published elsewhere, replacement of the guanines in the second case with inosines eliminates the anomalous behavior.

Crystals from the motif with the shortest sticky end (G:C) grown using the protocol above diffracted marginally better (4.75 \AA) than the original 2-nt (GA:TC) sticky end (4.9 \AA) at the same beamline. However, using a faster annealing protocol, in which the temperature of the crystal setup was brought from 60 to 20 $^{\circ}\text{C}$ in less than an hour, we were able to obtain 1-nt G:C crystals that diffracted to 3.4 \AA , while the 2-nt GA:TC crystals grown using this same procedure diffracted only to 4.85 \AA . Thus, a shorter sticky end gives a more favorable

contact for crystal self-assembly in this case. Comparison of fast and slow annealing of crystals is shown in Table 1. However, crystals grown using the fast annealing procedure had a higher mosaicity value. Each crystal is considered to be composed of mosaic blocks, with each block being a perfect crystal. If all blocks were completely aligned, the individual blocks would be exactly parallel and the mosaicity would be 0. However, the mosaic blocks are usually imperfectly aligned (even without perturbations, such as flash-cooling), making mosaicity one of the parameters that contributes to the quality of a crystal.

Crystals from 3-nt (GAG:CTC) sticky ends, grown using the protocol previously described, gave small crystals unsuitable for mounting. Changing the sequence of the 2-nt motif to AA:TT yielded crystals that diffracted to 4.63 \AA , and changing the 3-nt motifs to TAT:ATA and TAG:CTA produced better-sized crystals. The TAG:CTA crystals diffracted to 4.20 \AA (Figure S1) at the same beamline, comparatively better than the 2-nt GA:TC, which was 4.9 \AA . The sticky end sequence ATA:TAT often formed clusters leading to a poor diffraction pattern, with resolution of 6.00 \AA . 2-nt sticky ends CC:GG yielded crystals that diffracted to 6.50 \AA , while 2-nt sticky ends CC:II (I represents inosine, guanine without the 2-amino group) yielded crystals that diffracted to 4.70 \AA .

Finally while the 4-nt sticky-ends GAGC:GCTC gave small crystals unsuitable for mounting, the 4-nt sticky-ends

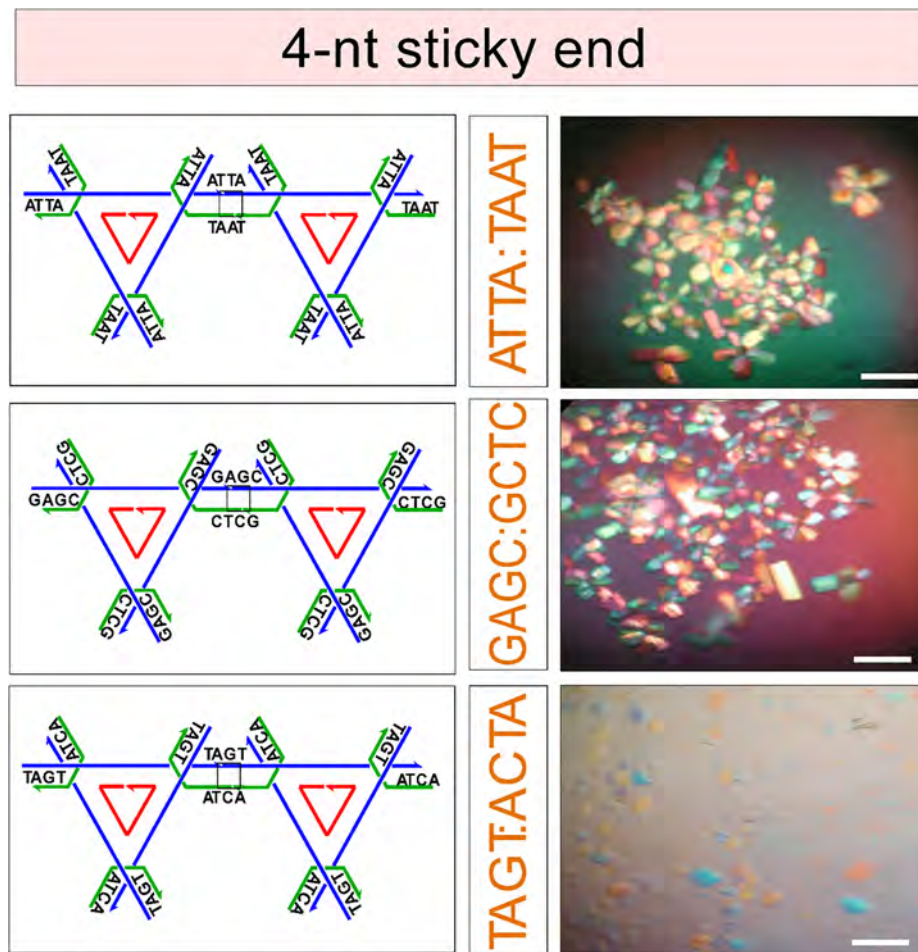


Figure 5. Crystals of the 2-turn triangle with 4-nucleotide sticky ends. The image shows the sticky end connectivity between two neighboring triangles (left) and the respective crystals obtained from the designs (right). Scale bars are 100 μ m.

Table 1. X-ray Data of Crystals Obtained from Slow and Fast Annealing Procedures^a

protocol	slow annealing (as in ref 7)		fast annealing
	60 °C \rightarrow 20 °C at 0.2 °C/h	60 °C \rightarrow 20 °C at 100 °C/h	
design	1-nt (G:C)	2-nt (GA:CT)	1-nt (G:C)
resolution (Å)	4.75	4.90	3.40
space group	R3	R3	R3
unit cell dimensions	$a = 68.59$ Å $\alpha = 103.63^\circ$	$a = 69.14$ Å $\alpha = 101.07^\circ$	$a = 69.42$ Å $\alpha = 101.33^\circ$
unit cell volume (Å ³)	289920	309193	311819
mosaicity (deg)	0.42–0.76	0.48–0.98	0.72–1.42

^aThe 2-nt sticky end design was grown using both procedures for comparison.

TAGT:ACTA yielded crystals that diffracted to 5.20 Å and 4-nt sticky-ends ATTAA:TAAT crystals diffracted to 5.50 Å. Table 2 shows a detailed comparison of sticky end length and sequence of crystals formed by the 2-turn triangle motif.

The designed motif is \sim 7 nm on each edge (2 helical turns of DNA) and self-assembles to form macroscopic three-dimensional crystals. For this to happen, the unit cells have to connect over and over again during crystal growth. If structures with different geometries are kinetically accessible, irregular assemblies may result rather than crystalline lattices.¹⁵ The

branched DNA motifs used in this construction are quite rigid, and association via the sticky ends is the only assembly process available during crystal assembly. Also, the short duplex sticky ends used in this design may also provide lower activation energies for breaking down imperfect structures in dynamic assembly/disassembly processes and are expected to lead more readily to the best-aligned crystal lattices. Thus, a shorter sticky end gives a more effective contact for crystal self-assembly. The 3-nt sticky ends TAG:CTA diffracted better than the 2-nt sticky ends at NSLS-I-X25. By employing longer sticky ends, the reversibility of the assembly could be achieved at a particular higher temperature at which the crystals form. This feature might make it useful in fractal assemblies of DNA and for DNA computation in three-dimensions.

Effect of 3'-Phosphates. 3'-Phosphates were added on all strands of triangles with 1-nt and 2-nt sticky ends and diffracted to 4.80 and 4.40 Å, respectively, better than the triangle without any phosphates. An optical image of crystals from the 2-nt GA:TC cohesive crystal containing 3'-phosphates on all strands is shown in Figure S2. Motifs containing both 5'- and 3'-phosphates on all strands were also crystallized (Figure S2) and diffracted to 5.15 Å. All structures were isomorphous with the original structure reported in ref 7 (Table 3).

Effect of Bases Flanking the Sticky End. The bases flanking the sticky ends may have a bearing on how effectively the sticky ends hold the lattice together because they affect the

Table 2. X-ray Data and Unit Cell Parameters of Crystals from 2-Turn Triangle Crystals Formed from Different Sticky End Length and Sequences

sticky end length and sequence	sticky-end sequence	beamline	space group	unit cell dimensions	resolution (Å)
G:C	NSLS-X25	R3		$a = 69.42 \text{ \AA}, \alpha = 101.33^\circ$	3.40
GA:TC	NSLS-X25	R3		$a = 69.14 \text{ \AA}, \alpha = 101.07^\circ$	4.80
TT:AA	NSLS-X25	R3		$a = 69.18 \text{ \AA}, \alpha = 102.47^\circ$	4.63
CC:GG	NSLS-X25	$P3_1$		$a = b = 68.97 \text{ \AA}, c = 179.90 \text{ \AA}, \alpha = \beta = 90.0^\circ, \gamma = 120.0^\circ$	5.90
CC:II	APS-19ID	R3		$a = 69.34 \text{ \AA}, \alpha = 100.90^\circ$	4.70
TG:CA	NSLS-X25	R3		$a = 69.22 \text{ \AA}, \alpha = 101.17^\circ$	4.20
TAG:CTA	NSLS-X25	R3		$a = 69.42 \text{ \AA}, \alpha = 100.80^\circ$	4.20
TAT:ATA	NSLS-X25	R3		$a = 68.0 \text{ \AA}, \alpha = 100.0^\circ$	5.60
GAG:CTC	NSLS-X25	R3		$a = 68.70 \text{ \AA}, \alpha = 102.34^\circ$	6.50
TAGT:ACTA	APS-19ID	R3		$a = 69.04 \text{ \AA}, \alpha = 100.8^\circ$	5.20
ATTA:TAAT	APS-19ID	R3		$a = 69.03 \text{ \AA}, \alpha = 102.11^\circ$	5.50

stacking of the ultimate nucleotide on the sticky end of the adjoining molecule. The 2-nucleotide sticky end GA:TC was modified to be flanked by GC base pairs and was crystallized (Figure S3). The resolution of the crystals formed from this motif was 4.09 Å, compared to 4.90 Å from the original motif (both at NSLS-I-X25) in which only one of the sticky ends was flanked by GC nucleotide pairs and the other was flanked by TA. Crystal resolution and unit cell parameters are shown in Table 4.

Since the 1-nt G:C sticky end diffracted better than the 2-nt sticky ends, the sequences of this motif were modified to have GC:GC base pairs flanking the sticky ends, and further, 5'-phosphates were added on all combinations of strands. However, the diffraction of these crystals was not better than those obtained previously with 5'-phosphates on 1-nt sticky ends (Table S1).

Effect of 5'-Phosphates Combinations. Triangles with 5'-phosphates were shown earlier to have a higher resolution when compared at NSLS-I-X25.¹³ In the previous study, 5'-phosphates were added on all strands involved in the formation of the motif. Here, the symmetric 2-turn tensegrity triangle

Table 4. X-ray Data and Unit Cell Parameters of Crystals from 2-Turn Triangle Crystals Formed from GC-Flanked 2-Nucleotide Sticky End

GC:GC base pair flanking the sticky end	sticky-end sequence	beamline	space group	unit cell dimensions	resolution (Å)
	C:G	NSLS-X25	R3	$a = 69.14 \text{ \AA}, \alpha = 101.66^\circ$	7.00
	C:G 5'-phosphate	NSLS-X25	R3	$a = 68.85 \text{ \AA}, \alpha = 102.09^\circ$	4.40
	GA:TC	NSLS-X25	R3	$a = 69.24 \text{ \AA}, \alpha = 101.22^\circ$	4.09

motif was crystallized with 5'-phosphates on combinations of strand 1, strand 2, and strand 3 in motifs with 1-nt (G:C) (Figure S4) and 2-nt (GA:TC) (Figure S5) sticky ends, thereby yielding 16 different crystals (Figures 6a and 6b). X-ray diffraction results of these 16 combinations at NSLS-I-X25 beamline are shown in Table 5. The best resolution for the 2-nt crystals was 4.09 Å (1-2-3P), which was equivalent to the previously reported resolution with 5'-phosphates on all three strands.¹³ Combinations 1-2P-3P, 1P-2-3, 1P-2P-3, and 1P-2P-3P for the 1-nt G:C motif diffracted between 3.0 and 3.2 Å at NSLS-I-X25 and 1P-2-3 diffracted to a nominal 2.62 Å (38% occupancy) resolution at APS-19ID; the mosaicity of the crystal was found to be 0.51–0.81°. This was the best resolution obtained for these self-assembled crystals. The structure was similar to that in ref 7 (PDB ID: 3GBI) and its PDB ID is 5W6W. Figure 6c shows the crystal structure with electron density of the 1nt:1P-2-3 at a nominal 2.62 Å resolution, and Figure 6d shows the comparison of refined structures from NSLS-I-X25 (red) and APS (green). Diffraction patterns for these crystals are shown in Figure 7. Data analysis and statistics for the 1-nt: 1P-2-3 crystal from APS and NSLS are detailed in Table 6. Attempts to extend the 1-nucleotide sticky end to a 0-nucleotide sticky did not yield the designed blunt-end cohering crystals.

For crystals produced with a thermal protocol, one might interpret the results above to suggest that the factors that lead to the crystals with the highest resolution should all cause the crystals to come out of solution at the lowest possible temperature. Thus, one might imagine that the repulsions owing to the phosphates and the weakness of the single-nucleotide interactions might cause the molecules to be less susceptible to structural fluctuations at the lower temperatures they require to self-assemble. An experiment to test this notion is the thermal assembly of a crystal with two molecules in the asymmetric unit that are not introduced to each other until the temperature is low. We have performed this experiment by forming the two molecules and cooling them to 4 °C before

Table 3. X-ray Data and Unit Cell Parameters of Crystals from 2-Turn Triangle Containing 5'-Phosphate or 3'-Phosphates

phosphate addition		beamline	space group	unit cell dimensions	resolution (Å)
sticky-end sequence					
5'-phosphate A:T	NSLS-X25	$P3_1$		$a = b = 128.2 \text{ \AA}, c = 62.12 \text{ \AA}, \alpha = \beta = 90.0^\circ, \gamma = 120.0^\circ$	5.80
5'-phosphate C:G	NSLS-X25	R3		$a = 68.85 \text{ \AA}, \alpha = 102.09^\circ$	4.40
5'- and 3'-phosphate C:G	NSLS-X25	R3		$a = 69.05 \text{ \AA}, \alpha = 101.46^\circ$	4.74
5'-phosphate GA:TC	NSLS-X25	R3		$a = 69.08 \text{ \AA}, \alpha = 101.35^\circ$	4.40
3'-phosphate GA:TC	NSLS-X25	R3		$a = 68.91 \text{ \AA}, \alpha = 101.40^\circ$	4.40
5'- and 3'-phosphate GA:TC	NSLS-X25	R3		$a = 69.17 \text{ \AA}, \alpha = 101.57^\circ$	6.45

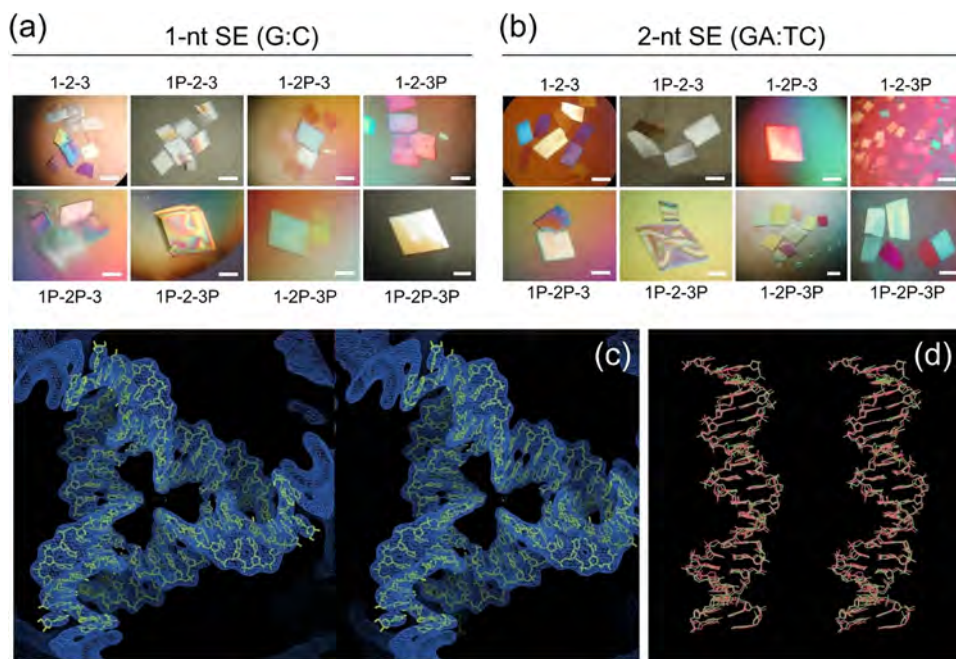


Figure 6. Optical images of crystals with 5'-phosphates combinations. 5'-Phosphate was added to one, two, or all three strands in (a) 1-nucleotide and (b) 2-nucleotide sticky end triangles, yielding 16 different crystals. The addition of 5'-phosphate to strands is denoted by P. Scale bars are 100 μ m. (c) Stereographic projection of the refined model from 1-nt 1P-2-3 crystal flanked by its electron density. This image shows the whole triangle structure (three asymmetric units) refined by molecular replacement from modified coordinates of 3GBI. The electron density map is contoured at 1.5 sigma. Note this image is based on the best diffracting crystal encountered in this study. (d) Asymmetric unit (one duplex edge) of the data from NSLS (red) and APS (green) superimposed on to each other. There is virtually no difference.

Table 5. X-ray Data, Unit Cell Parameters, and Mosaicity of Crystals from 2-Turn Triangle Crystals with 5'-Phosphates on Different Strand Combinations

effect of 5'-phosphates on DNA strands in a 2-turn symmetric motif						
5'-P position	1-nucleotide sticky-end (G:C)			2-nucleotide sticky-end (GA:TC)		
	resolution (Å)	unit cell (R3)	mosaicity (deg)	resolution (Å)	unit cell (R3)	
1-2-3	3.40	$a = 69.65 \text{ \AA}$ $\alpha = 100.77^\circ$	1.26–1.84	4.85	$a = 69.06 \text{ \AA}$ $\alpha = 101.63^\circ$	
1P-2-3	2.62 (APS-19ID)	$a = 69.14 \text{ \AA}$ $\alpha = 101.03^\circ$	0.36–0.89	4.80	$a = 69.14 \text{ \AA}$ $\alpha = 102.22^\circ$	
1-2P-3	5.20	$a = 69.34 \text{ \AA}$ $\alpha = 101.16^\circ$	0.78–1.32	4.80	$a = 69.06 \text{ \AA}$ $\alpha = 101.89^\circ$	
1-2-3P	4.90	$a = 69.58 \text{ \AA}$ $\alpha = 100.79^\circ$	0.51–0.96	4.10	$a = 69.27 \text{ \AA}$ $\alpha = 101.33^\circ$	
1P-2P-3	3.20	$a = 68.98 \text{ \AA}$ $\alpha = 102.27^\circ$	0.93–1.60	4.40	$a = 69.24 \text{ \AA}$ $\alpha = 101.88^\circ$	
1P-2-3P	4.80	$a = 68.96 \text{ \AA}$ $\alpha = 101.25^\circ$	1.04–2.21	5.20	$a = 69.44 \text{ \AA}$ $\alpha = 101.33^\circ$	
1-2P-3P	3.00	$a = 68.50 \text{ \AA}$ $\alpha = 100.89^\circ$	0.92–3.31	5.10	$a = 69.32 \text{ \AA}$ $\alpha = 101.60^\circ$	
1P-2P-3P	3.10	$a = 69.18 \text{ \AA}$ $\alpha = 101.26^\circ$	0.76–1.30	4.40	$a = 69.08 \text{ \AA}$ $\alpha = 101.35^\circ$	

allowing them to interact. Unfortunately, this experiment did not give crystals that diffracted well at all. The crystals diffracted to 5.65 Å; in contrast, the originally crystallized two-component crystal with 2-nucleotide sticky ends diffracted to 5.00 Å at a weaker beamline.⁸ Thus, this hypothesis seems to be incorrect.

CONCLUSIONS

A key goal of DNA nanotechnology is to find a rational solution to the crystallization problem of biological macro-

molecules for purposes of determining guest structures by X-ray diffraction.³ We have crystallized tensegrity triangle motifs with variable sticky end lengths and sequences that diffract much better than the originally reported structure. This length of sticky ends is quite unusual compared to that used in attempts to obtain supramolecular lattices,¹⁶ DNA-based assemblies of nanoparticles,¹⁵ and for nanoconstruction in general.^{17–19} We have also shown that the addition of 5'-phosphates on one, two, or all three strands of the tensegrity triangle favorably affects the resolution of the self-assembled

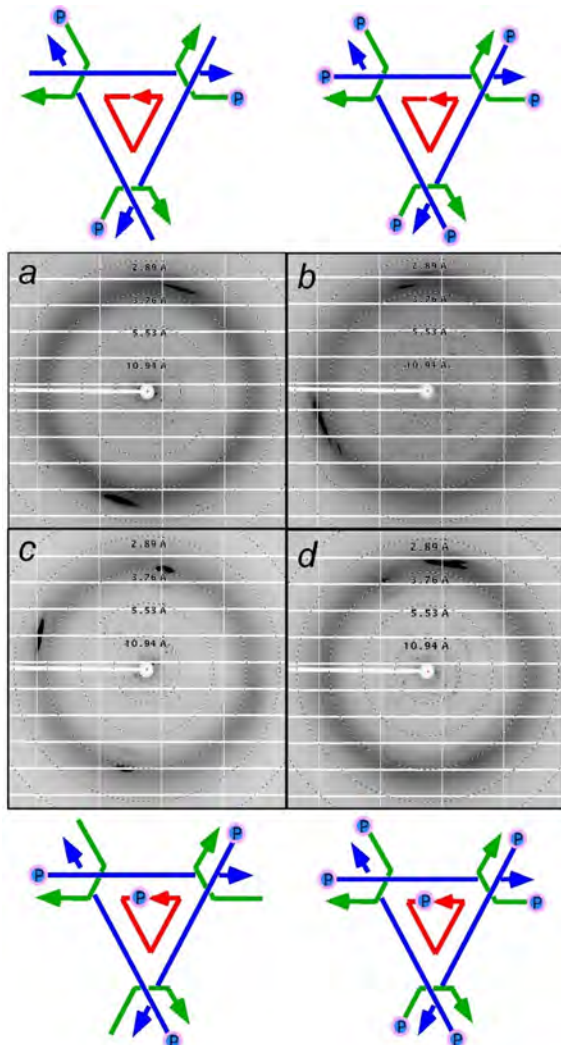


Figure 7. Diffraction patterns of crystals obtained from 1-nucleotide sticky ends. (a) 1P-2-3, (b) 1P-2P-3, (c) 1-2P-3P, and (d) 1P-2P-3P. 'P' denotes the position of 5'-phosphate.

crystals and that 1-nt sticky ends with 5'-phosphates yield the best resolution. We also tested the addition of 3'-phosphates on the strands and both 5' and 3' phosphates addition. Overall, we found no correlation between the strength of the sticky ends²⁰ and the quality of the crystals. This improvement in resolution of the designed lattices might lead to this lattice being used as a framework to host small macromolecular guests. Larger motifs with bigger cavity sizes, such as triangles with 3- and 4-helical turns per edge, would be more suitable for more typically sized macromolecules.

METHODS

Synthesis and Purification of DNA. All DNA molecules in this study have been synthesized on an Applied Biosystems 394 automatic DNA synthesizer, removed from the support, and deprotected, using routine phosphoramidite procedures. DNA strands were purified by denaturing polyacrylamide gel electrophoresis containing 6–20% acrylamide (19:1 acrylamide/bisacrylamide). Bands corresponding to DNA strands of expected size were excised from denaturing gels stained with ethidium bromide. DNA was eluted in a solution containing 500 mM ammonium acetate, 10 mM magnesium acetate, and 1 mM EDTA at 4 °C overnight. The eluates were then extracted with butanol to remove ethidium, and the DNA was recovered by ethanol precipitation. The amount of DNA was estimated by OD260.

Table 6. Data Analysis and Refinement Statistics for 1SE:1P-2-3 at APS and NSLS^a

data and refinement statistics for 2-turn 1-nt SE:1P-2-3 PDB ID: 5W6W		
space group	R3	R3
cell constants $a = b = c$, $\alpha = \beta = \gamma$	$a = 69.26 \text{ \AA}$, $\alpha = 100.82^\circ$	$a = 69.13 \text{ \AA}$, $\alpha = 101.03^\circ$
resolution (Å)	20.39–2.62	32.96–3.06
% data completeness (resolution range)	39.2 (20.39–2.62)	68.0 (32.96–3.06)
R_{merge}	0.090	0.107
$\langle I/\sigma(I) \rangle$	1.13 (at 2.63 Å)	1.56 (at 3.06 Å)
mosaicity	0.51–0.81	0.37–0.91
$R_{\text{work}}/R_{\text{free}}$	0.195/0.260 (0.213/0.276) ^b	0.207/0.236 (0.200/0.233) ^b
R_{free} test set	479 reflections (11.22%)	452 reflections (10.05%)
rms bonds (Å), rms angles (deg)	0.013, 1.637	0.011, 1.180
Wilson B-factor (Å)	121.9	86.9
anisotropy	0.418	0.627
bulk solvent k_{sol} (e/Å ³), B_{sol} (Å ²)	0.10, 39.8	0.10, 39.2
estimated twinning fraction	0.053 for h, h-k, l	0.045 for h, h-k, l
L-test for twinning	$\langle L \rangle = 0.46$, $\langle L^2 \rangle = 0.28$	$\langle L \rangle = 0.48$, $\langle L^2 \rangle = 0.30$
$F_{\text{o}}F_{\text{c}}$ correlation	0.98	0.97
total number of atoms	859	855
average B, all atoms (Å ²)	143.0	173.0
estimated coordinate error (Å ²)	0.24	0.38
collecting beamline	APS beamline 19ID	NSLS-I beamline X25

^aIn both cases, a complete sphere of native X-ray data was collected at 1° wedges. ^bNumbers in parentheses represent values for the highest resolution bin.

Crystallization. Crystals were grown from 5 μL hanging drops in a thermally controlled incubator containing 25 μM DNA, 40 mM Tris, 2 mM EDTA, 20 mM acetic acid, 125 mM magnesium acetate, and 583 mM ammonium sulfate equilibrated against a 600 μL reservoir containing 120 mM Tris, 6 mM EDTA, 60 mM acetic acid, 375 mM magnesium acetate, and 1.75 M ammonium sulfate. Crystals were obtained by slow annealing, in which the temperature was decreased from 60 °C to room temperature (20 °C) or 4 °C with a cooling rate of 0.4 °C per hour. For the fast annealing protocol, crystals were grown in buffer containing 6 μM DNA, 40 mM Tris, 2 mM EDTA, 20 mM acetic acid, 125 mM magnesium acetate, and equilibrated against a 600 μL reservoir of 1.75 M ammonium sulfate. The setup was cooled from 60 to 20 °C at 100 °C per hour. Crystals were obtained at the end of the cooling step, and appeared full-sized within a day.

Data Collection and Structure Solution. Crystals were transferred to a cryosolvent of 30% glycerol, 28 mM Tris, 1.4 mM EDTA, 14 mM acetic acid, 87.5 mM magnesium acetate, and were frozen by immersion into liquid nitrogen. X-ray diffraction data were collected at 1.1 Å on beamline X25 at the National Synchrotron Light Source (Brookhaven National Laboratory, Upton, New York, USA). The diffraction data were processed in space group R3 using HKL-2000²¹ and the structure was determined *via* molecular replacement using PHENIX program package,²² and the search model was the previously determined DNA triangle structure (PDB code 3GBI).

ASSOCIATED CONTENT

Supporting Information

The Supporting Information is available free of charge on the ACS Publications website at DOI: 10.1021/acs.nano.9b02430.

Electron density map of 2-turn 3-nt TAG:CTA crystals; structural diagrams and crystals of various motifs; X-ray diffraction data at NSLS-X25 of crystals from 1-nt G:C SE with GC:GC base pairs flanking the sticky ends; 5'-phosphates added on combinations of one, two, or all three strands involved in formation of the triangle (PDF)

AUTHOR INFORMATION

Corresponding Author

*E-mail: ned.seeman@nyu.edu.

ORCID

Arun Richard Chandrasekaran: [0000-0001-6757-5464](https://orcid.org/0000-0001-6757-5464)

Ruojie Sha: [0000-0002-0807-734X](https://orcid.org/0000-0002-0807-734X)

Philip S. Lukeman: [0000-0003-0563-5032](https://orcid.org/0000-0003-0563-5032)

Chengde Mao: [0000-0001-7516-8666](https://orcid.org/0000-0001-7516-8666)

Nadrian C. Seeman: [0000-0002-9680-4649](https://orcid.org/0000-0002-9680-4649)

Notes

The authors declare no competing financial interest.

ACKNOWLEDGMENTS

We acknowledge support of the following grants to N.C.S.: Grant No. GM-29554 from NIGMS, Grant Nos. CTS-1120890, CCF-1117210, EFRI-1332411, and CHE-1708776 from the NSF, Grant No. W911NF-1110024 from ARO, Grant Nos. N000141110729 and N000140911118 from ONR, DE-SC0007991 from DOE for DNA synthesis, and partial salary support and GBMF3849 from the Gordon and Betty Moore Foundation. Use of the National Synchrotron Light Source, Brookhaven National Laboratory, was supported by the U.S. Department of Energy, Office of Science, Office of Basic Energy Sciences, under Contract No. DE-AC02-98CH10886.

REFERENCES

- Watson, J. D.; Crick, F. H. C. Molecular Structure of Nucleic Acids: A Structure for Deoxyribose Nucleic Acid. *Nature* **1953**, *171*, 737–738.
- Seeman, N. C. DNA in a Material World. *Nature* **2003**, *421*, 427–431.
- Seeman, N. C. Nucleic Acid Junctions and Lattices. *J. Theor. Biol.* **1982**, *99*, 237–247.
- Seeman, N. C. Macromolecular Design, Nucleic Acid Junctions, and Crystal Formation. *J. Biomol. Struct. Dyn.* **1985**, *3*, 11–34.
- Qiu, H.; Dewan, J. C.; Seeman, N. C. A DNA Decamer with A Sticky End: the Crystal Structure of d-CGACGATCGT. *J. Mol. Biol.* **1997**, *267*, 881–898.
- Liu, D.; Wang, W.; Deng, Z.; Walulu, R.; Mao, C. Tensegrity: Construction of Rigid DNA Triangles with Flexible Four-Arm DNA Junctions. *J. Am. Chem. Soc.* **2004**, *126*, 2324–2325.
- Zheng, J.; Birktoft, J. J.; Chen, Y.; Wang, T.; Sha, R.; Constantinou, P. E.; Ginell, S. L.; Mao, C.; Seeman, N. C. From Molecular to Macroscopic via the Rational Design of a Self-Assembled 3D DNA Crystal. *Nature* **2009**, *461*, 74–77.
- Wang, T.; Sha, R.; Birktoft, J. J.; Zheng, J.; Mao, C.; Seeman, N. C. A DNA Crystal Designed to Contain Two Molecules per Asymmetric Unit. *J. Am. Chem. Soc.* **2010**, *132*, 15471–15473.
- Nguyen, N.; Birktoft, J. J.; Sha, R.; Wang, T.; Zheng, J.; Constantinou, P. E.; Ginell, S. L.; Chen, Y.; Mao, C.; Seeman, N. C. The Absence of Tertiary Interactions in a Self-Assembled DNA Crystal Structure. *J. Mol. Recognit.* **2012**, *25*, 234–237.
- Egli, M. "Deoxyribo Nanonucleic Acid"; Antiparallel, Parallel, and Unparalleled. *Chem. Biol.* **2004**, *11*, 1027–1029.
- Paukstelis, P. J.; Nowakowski, J.; Birktoft, J. J.; Seeman, N. C. Crystal Structure of a Continuous Three-Dimensional DNA Lattice. *Chem. Biol.* **2004**, *11*, 1119–1126.
- Robinson, B. H.; Seeman, N. C. The Design of a Biochip: a Self-Assembling Molecular-Scale Memory Device. *Protein Eng., Des. Sel.* **1987**, *1*, 295–300.
- Sha, R.; Birktoft, J. J.; Nguyen, N.; Chandrasekaran, A. R.; Zheng, J.; Zhao, X.; Mao, C.; Seeman, N. C. Self-Assembled DNA Crystals: The Impact on Resolution of 5'-Phosphates and the DNA Source. *Nano Lett.* **2013**, *13*, 793–797.
- Stahl, E.; Praetorius, F.; de Oliveira Mann, C. C.; Hopfner, K. P.; Dietz, H. Impact of Heterogeneity and Lattice Bond Strength on DNA Triangle Crystal Growth. *ACS Nano* **2016**, *10*, 9156–9164.
- Nykypanchuk, D.; Maye, M. M.; van der Lelie, D.; Gang, O. DNA-Guided Crystallization of Colloidal Nanoparticles. *Nature* **2008**, *451*, 549–552.
- Stewart, K. M.; Rojo, J.; McLaughlin, L. W. Ru(II) Tris(bipyridyl) Complexes with Six Oligonucleotide Arms as Precursors for the Generation of Supramolecular Assemblies. *Angew. Chem.* **2004**, *116*, 5808–5811.
- Zhao, Z.; Liu, Y.; Yan, H. Organizing DNA Origami Tiles into Larger Structures Using Preformed Scaffold Frames. *Nano Lett.* **2011**, *11*, 2997–3002.
- Liu, W.; Zhong, H.; Wang, R.; Seeman, N. C. Crystalline Two-Dimensional DNA Origami Arrays. *Angew. Chem., Int. Ed.* **2011**, *50*, 264–267.
- Zhang, T.; Hartl, C.; Frank, K.; Heuer-Jungermann, A.; Fischer, S.; Nickels, P. C.; Nickel, B.; Liedle, T. 3D DNA Origami Crystals. *Adv. Maters.* **2018**, *30*, 1800273.
- SantaLucia, J. A Unified View of Polymer, Dumbbell and Oligonucleotide DNA Nearest-Neighbor Thermodynamics. *Proc. Natl. Acad. Sci. U. S. A.* **1998**, *95*, 1460–1465.
- Otwinowski, Z.; Minor, W. Processing of X-Ray Diffraction Data Collected in Oscillation Mode. *Methods Enzymol.* **1997**, *276*, 307–326.
- Adams, P. D.; Afonine, P. V.; Bunkoczi, G.; Chen, V. B.; Davis, I. W.; Echols, N.; Headd, J. J.; Hung, L. W.; Kapral, G. J.; Grosse-Kunstleve, R. W.; McCoy, A. J.; Moriarty, N. W.; Oeffner, R.; Read, R. J.; Richardson, D. C.; Richardson, J. S.; Terwilliger, T. C.; Zwart, P. H. PHENIX: a Comprehensive Python-Based System for Macromolecular Structure Solution. *Acta Crystallogr., Sect. D: Biol. Crystallogr.* **2010**, *D66*, 213–221.